Magnetic dipole band in ^{124}Xe

I. Schneider,[1] R. S. Chakrawarthy,[1] I. Wiedenhöver,[1] A. Schmidt,[1] H. Meise,[1] P. Petkov,[1,4] A. Dewald,[1] P. von Brentano,[1] O. Stuch,[1] K. Jessen,[1] D. Weisshaar,[1] C. Schumacher,[1] O. Vogel,[1] G. Sletten,[2] B. Herskind,[2] M. Bergström,[2] and J. Wrzesinski[3]

[1]*Institut für Kernphysik der Universität zu Köln, D-50937 Köln, Germany*

[2]*Niels-Bohr-Institute, Tandem Accelerator Laboratory, Risø, DK-4000 Roskilde, Denmark*

[3]*Institute of Nuclear Research, Krakow, Poland*

[4]*Bulgarian Academy of Sciences, Institute for Nuclear Research and Nuclear Energy, 1784 Sofia, Bulgaria*

(Received 21 July 1998; published 16 June 1999)

High-spin states in ^{124}Xe were populated in the fusion-evaporation reaction ^{110}Pd(^{18}O,4n)^{124}Xe at a beam energy of 86 MeV. The experiment was performed at the NORDBALL spectrometer in Risø, Denmark. The decay out of a magnetic dipole band was established for the first time in this nucleus. By means of angular correlations from oriented states the multipole mixing ratios for 9 of the 12 gamma transitions of the magnetic dipole band were deduced. The experimental $B(M1;I\rightarrow I-1)/B(E2;I\rightarrow I-2)$ values were compared to estimates of the Dönau-Frauendorf semiclassical model. The dipole band is inferred to be based on a prolate four-quasiparticle configuration of the type $[\nu(h_{11/2}\otimes g_{7/2})]\otimes[\pi(h_{11/2}\otimes d_{5/2}/g_{7/2})]$. [S0556-2813(99)01708-2]

PACS number(s): 21.10.Re, 27.60.+j, 23.20.En, 23.20.Lv

I. INTRODUCTION

In recent years much interest has been focused on the study of dipole bands near the $Z=82$ and $Z=50$ shell closures [1–4]. The interesting new aspect of these bands is that the total angular momentum is tilted relative to the principal axis of the deformed nucleus [5,6]. This occurs due to large spin components of the constituent quasiparticles onto the conventional axis of rotation and the symmetry axis. These bands are known as the tilted (t) bands. The tilted axis cranking model suggests a novel mechanism to generate dipole bands in the weakly deformed Sn and Pb nuclei [5,6]. In this mechanism, the configurations of the dipole bands are based on high-j proton particles (holes) and neutron holes (particles). The angular momentum vectors are approximately perpendicular at the bandhead. As a result of Coriolis force, the closing (or shearing) of these two high-j vectors results in states of higher angular momentum. The mechanism to generate these bands is called the ''shears mechanism.'' Interestingly, in the middle of a high-j shell, where pairing and quadrupole deformation is significant, the Coriolis effect results in a Fermi-aligned coupling scheme (as in ^{179}W [7]). A detailed description of ''shears bands'' and ''t bands'' can be found in Ref. [6]. In general, the $B(M1)$ strengths in dipole bands depend on the configuration of the underlying structure. These are larger when protons are involved and also for a large K value. Tilted axis cranking calculations also predict the existence of t bands in the $A\sim 130$ region [8]. The related particle-hole configurations are due to oblate neutron holes in the $h_{11/2}$ orbital coupled to proton particles in the $(h_{11/2}\otimes d_{5/2})$ orbitals. Since nuclei in this region have a larger deformation compared to the ones in the Pb region, it is interesting if the shears mechanism also plays an important role in the mass region $A\sim 130$ [2,6]. In the mass region $A\sim 130$, $\Delta I=1$ bands were observed in ^{122}Ba [9], ^{126}Ba [10], ^{128}Ba [11], and ^{126}Xe [12]. These bands are characterized by large $B(M1;I\rightarrow I-1)/B(E2;I\rightarrow I-2)$ values. Of the known dipole bands in the even-even Xe and Ba nuclei, only in ^{128}Ba have the gamma transitions linking the dipole band to lower-lying states been observed with an experiment recently performed at the GASP spectrometer of the INFN Legnaro, Italy [11]. Therefore only for the dipole band in ^{128}Ba are reliable values for the excitation energies and spins known to date.

In the present paper we show that the description of the dipole band in ^{124}Xe in terms of high-K rotational structures adequately explains all properties that have been measured to date and more exotic descriptions in terms of ''shears bands'' or ''t bands'' may not be required. Accurate data on $E2/M1$ mixing ratios, $B(M1;I\rightarrow I-1)/B(E2;I\rightarrow I-2)$ ratios, and the excitation energies and spins should provide a test to see if the high-K description breaks down at any point. With this motivation an experiment was performed to search for a dipole band and its linking transitions in ^{124}Xe.

II. EXPERIMENTAL DETAILS

High-spin states in ^{124}Xe were populated with the reaction ^{110}Pd(^{18}O,4n)^{124}Xe at a beam energy of 86 MeV. The experiment was performed at the NORDBALL spectrometer of the Niels-Bohr-Institute in Risø, Denmark. The NORDBALL spectrometer has been described in many publications (e.g., Ref. [13]). In the present experiment it consisted of an array of 20 Compton-suppressed hyperpure germanium (HPGe) detectors and a 4π barium fluoride (BaF_2) calorimeter. The calorimeter was equipped with 60 BaF_2 detectors. The target consisted of a 1 mg/cm^2 thick ^{110}Pd foil (enriched to 97.7%) backed onto a 3 mg/cm^2 thick tantalum foil. A total of 10^9 $\gamma\gamma$-coincidence events were accumulated. About 10% of the data set contained triple gamma coincidence events. The data were calibrated using radioactive sources of ^{152}Eu, ^{134}Cs, and ^{133}Ba. In the first step of the data analysis the gain-matched data were sorted into a $4k\otimes 4k$ coincidence matrix. The $4n$ reaction channel was enhanced in this matrix by using the average sum energy and

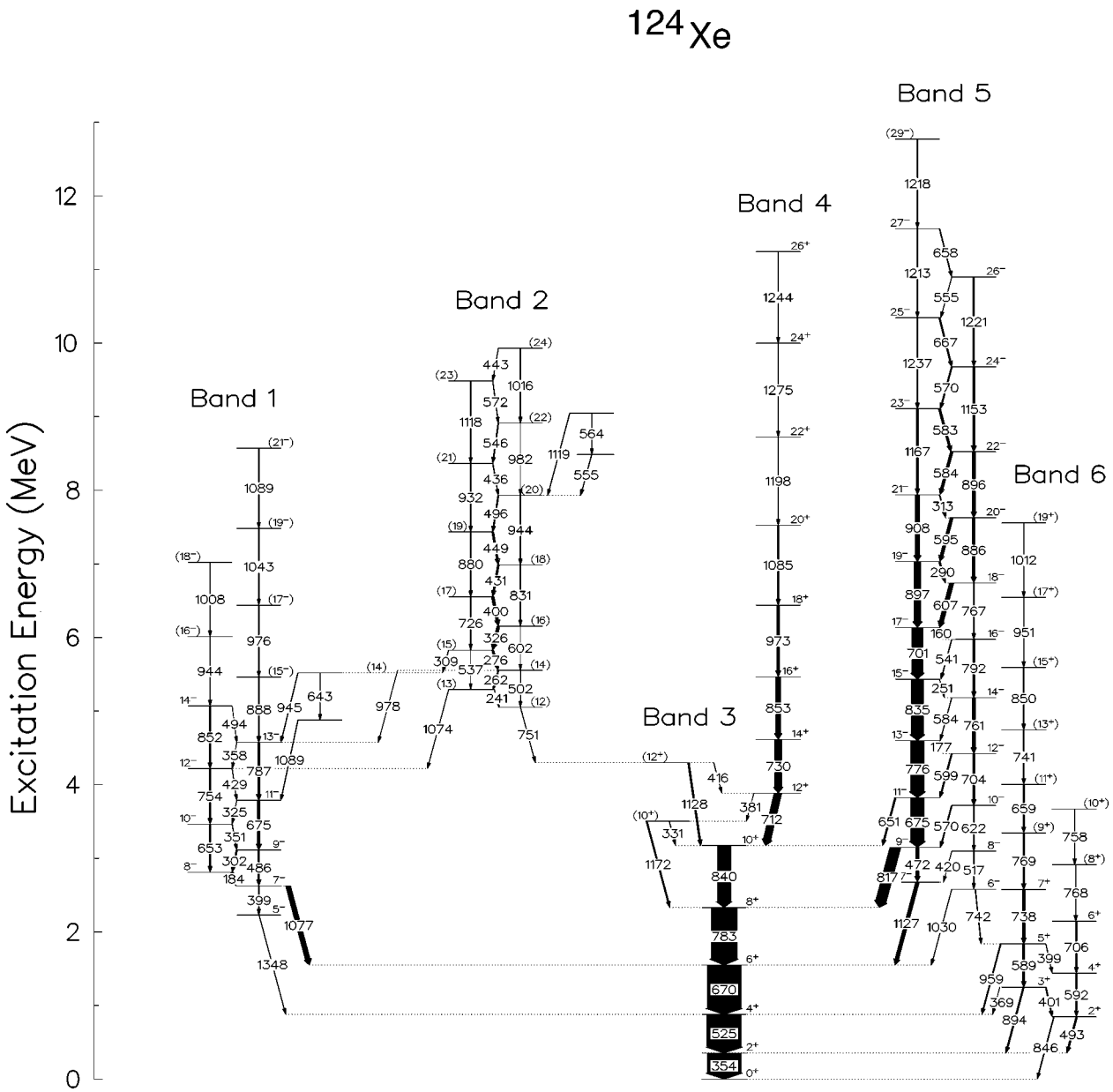

FIG. 1. The level scheme of ^{124}Xe from the present experiment. The gamma transition energies are marked in keV.

gamma multiplicity obtained from the 4π γ calorimeter to suppress the $5n$ reaction channel. At the chosen beam energy the data contained mainly ^{123,124}Xe events. Other weakly populated nuclei were ^{122}Xe and ^{123}I.

III. EXPERIMENTAL RESULTS

Figure 1 depicts the level scheme of ^{124}Xe obtained in the present work. In comparison to the earlier work [14], 42 new states and 82 new gamma transitions were established. Part of this work has been reported earlier [15]. While this paper was in preparation Bianco *et al.* have also reported independently the observation of a dipole band in ^{124}Xe [16]. In the present work, in addition, we were able to find gamma transitions linking the dipole band to the known states and the $E2/M1$ mixing ratio for the $\Delta I=1$ gamma transitions was deduced. The following discussion is restricted to the dipole band (band 2). The discussion of the other observed bands will be reported elsewhere.

The observed dipole band in ^{124}Xe is similar to the ones in the neighboring nuclei. It is connected to the ground state band and a negative parity band via gamma transitions of energies around 1 MeV; hence the absolute excitation energies of the levels of the band have been established. Figure 2(a) shows the $\Delta I=1$ (predominantly $M1$) gamma transitions of the dipole band spectrum gated by the 276 keV gamma transition of the band. The crossover $E2$ gamma transitions are shown in Fig. 2(b). In the same figure the linking gamma transitions are highlighted. Figure 3 shows the spectrum gated by the 1074 keV gamma transition, which is involved in the decay out of the dipole band. Weak but direct gamma decays to the negative parity band proceed

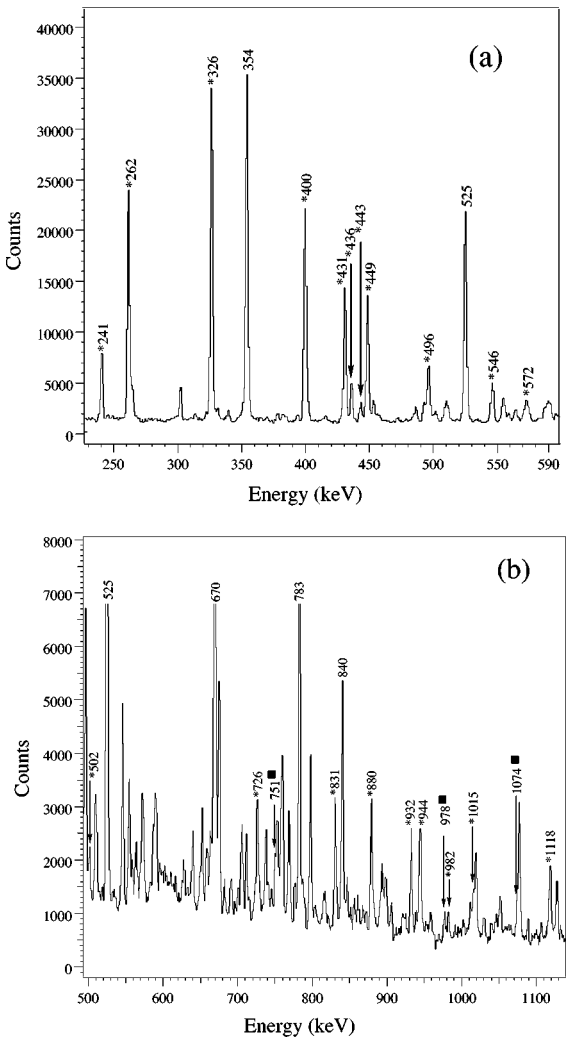

FIG. 2. Coincidence spectrum of the 276 keV gamma transition of the dipole band. (a) shows the $\Delta I=1$ (predominantly $M1$) gamma transitions (marked with an asterisk) and (b) shows the $E2$ crossover gamma transitions (marked with an asterisk) and the linking transitions (marked with a filled square).

via the 1074 and 978 keV gamma transitions. In addition, two-step decays were found to proceed via the coincident sequence of the 309 and 945 keV gamma transitions. The observed decays to the negative parity band account for about 40% of the intensity of the dipole band. Direct decay to the ground state band proceeds via the 751 keV gamma transition. Other gamma transitions (not shown in the level scheme) which were in coincidence with the dipole band have energies of 760, 1465, 1365, and 1020 keV. These gamma transitions could possibly be involved in the decay out of the dipole band, but they do not directly populate the ground state band (band 3) or the negative parity band (band 1). Because of their weaker intensity and contamination, they could not be placed in the level scheme. In the triples data set, these possible linking gamma transitions were very weak. The decay paths shown in the level scheme account for about 50% of the dipole band intensity.

The in-band gamma transitions in the dipole band are primarily $M1$ and $E2$. If we assume that the decay out does not

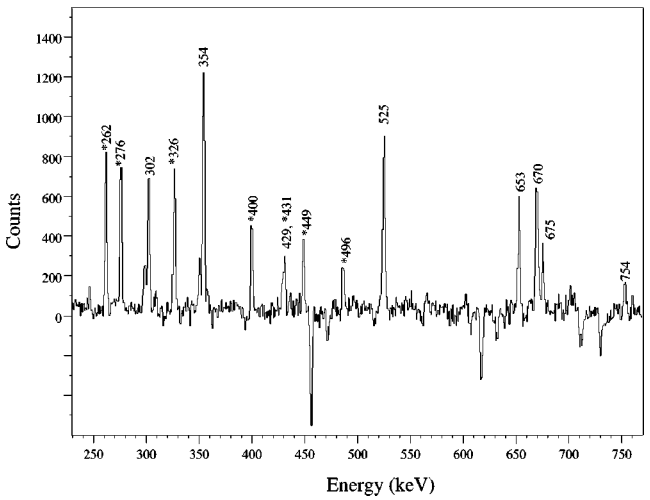

FIG. 3. Coincidence spectrum of the 1074 keV linking gamma transition involved in the decay out of the dipole band.

proceed via high multipolarity transitions ($L\geqslant 3$), then the spin values can be determined within $\pm 2\hbar$. The band starts at an energy of 5050 keV with a spin of $(12\pm 2)\hbar$ and the highest member of the band, observed in this experiment, has an excitation energy of 9929 keV and a spin value of $(24\pm 2)\hbar$. In the spectrum gated by the 354 keV $2^+\rightarrow 0^+$ gamma transition of the ground state band, the intensity of the strongest $\Delta I=1$ gamma transition (the 326 keV gamma transition) of the dipole band is about 13% of the intensity of the 525 keV $4^+\rightarrow 2^+$ transition of the ground band.

The 20 germanium detectors in the NORDBALL array are located in the hexagon positions of a truncated icosahedron with 12 pentagon and 20 hexagonal surfaces. This yields rings with 5 detectors equidistantly placed in each, with an azimuthal difference in ϕ of $360°/5=72°$. The rings are located at $\theta=37°$, 72°, 101°, and 143° with respect to the beam direction. The 190 combinations of any two detectors can be grouped into 9 different correlation groups using the high degree of symmetry of the setup [13]. In the second step of the data analysis, the coincidence events were sorted into 9 different angular correlation matrices corresponding to the 9 different groups (see Table I). Matrices resulting from 6 of these groups are symmetric and 3 of them are asymmetric. With the angular correlation information obtained from the correlation matrices it was possible to determine the spin differences ΔI and the $E2/M1$ multipole mixing ratios, δ, for 9 of the 12 gamma transitions in the dipole band. These mixing ratios vary from $\delta=-0.14\pm 0.03$ at the lowest spins to $\delta=-0.28\pm 0.07$ at the highest spins (see Table II). We adopt the sign convention given in Krane and Steffen [17]. As an example the correlation intensities for the coincident sequence of the 326 keV and 276 keV gamma transitions of the dipole band are shown in Fig. 4. As can be seen in the figure, the measured intensities for the different correlation groups show strong variations. Furthermore, in Fig. 4 the experimental data is compared to calculated values, resulting from fits with spin hypotheses $(16\rightarrow 15\rightarrow 14)$ and $(16\rightarrow 16\rightarrow 14)$. For each fit, the multipole mixing ratios of both the gamma transitions and the parameter σ were varied, while

TABLE I. Correlation groups of the Nordball spectrometer.

θ_1	θ_2	$\Delta\phi$	Correlation group	No. of detector pairs
37	37	72	1	5
143	143	72	1	5
143	37	108	1	10
37	37	144	2	5
143	143	144	2	5
143	37	36	2	10
37	79	0	3	5
143	101	0	3	5
143	79	180	3	5
37	101	180	3	5
37	79	72	4	10
143	101	72	4	10
143	79	108	4	10
37	101	108	4	10
37	79	144	5	10
143	101	144	5	10
143	79	36	5	10
37	101	36	5	10
37	143	180	6	5
79	79	72	7	5
101	101	72	7	5
101	79	108	7	10
79	79	144	8	5
101	101	144	8	5
101	79	36	8	10
79	101	180	9	5

the spin values of the levels were kept fixed. The fit for the $(16\rightarrow15\rightarrow14)$ spin hypothesis reproduces the experimental values very well (the resulting χ^2 is 1.3), whereas with the $(16\rightarrow16\rightarrow14)$ fit a poor agreement is achieved ($\chi^2=74.3$). The $(16\rightarrow15\rightarrow14)$ fit gives $\delta=-0.14$ for both multipole mixing ratios and a value of 1 for the parameter σ. A similar analysis for the 309 keV decay out gamma transition shows that it is a $\Delta I=1$ transition. This kind of analysis could not be performed for the transitions linking the dipole band to the lower-lying levels due to their weak intensities and contaminations in the angular correlation matrices.

TABLE II. $E2/M1$ mixing ratios of the dipole band.

E_γ [keV]	δ
241	-0.14 ± 0.03
262	-0.14 ± 0.03
276	-0.14 ± 0.03
326	-0.14 ± 0.03
400	-0.14 ± 0.03
431	-0.17 ± 0.04
449	-0.21 ± 0.03
496	-0.17 ± 0.03
436	-0.28 ± 0.07
309	-0.17 ± 0.03

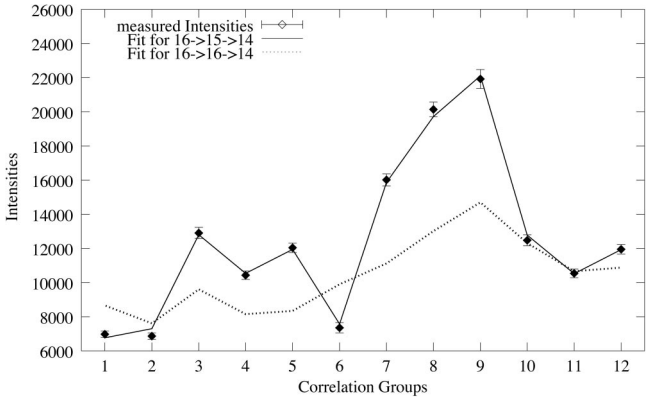

FIG. 4. Measured and calculated correlation intensities for the 326-276 keV cascade of the dipole band. The correlation group numbers refer to different combinations of the angles in the NORDBALL array. The group numbers 3, 4, and 5 together with those at 10, 11, and 12 are the ones for the three asymmetric matrices. The measured intensities are plotted with error bars. The values joined by the solid line result from a fit for a $(16\rightarrow15\rightarrow14)$ spin hypotheses and those joined by a dashed line result from a fit for a $(16\rightarrow16\rightarrow14)$ spin hypotheses.

IV. DISCUSSION

The dipole band shows no signature splitting up to a spin value of $(20\hbar)$. At higher spins a small signature splitting (and inversion) is observed, possibly due to quasiparticle alignment. The band has a large initial alignment (Fig. 5), which could be associated with a large contribution from quasiparticles. We restrict the following discussion on the interesting angular momentum dependence of the branching

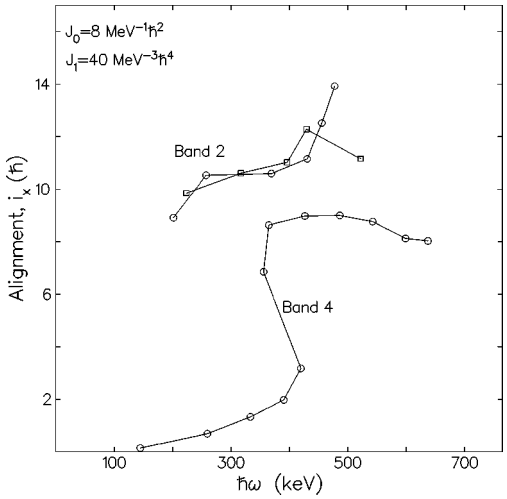

FIG. 5. The alignment plot of the ground state band and both signatures of the dipole band. The chosen Harris parameters are given in the figure.

ratios. It is well known that the magnitudes of the collective $B(M1;I\rightarrow I-1)$ reduced transition probabilities depend sensitively on the underlying intrinsic configuration. The $B(M1;I\rightarrow I-1)$ values are usually larger when protons are involved in the $M1$ transitions. Even when the absolute $B(M1)$ rates are not known, the branching ratios often can give crucial structural information. Thus, we have used the extended Dönau-Frauendorf geometric model [18] to make a configuration assignment for the dipole band. The following expression was employed to estimate the $B(M1)$ transition probablities:

$$B(M1;I\rightarrow I-1)=\frac{3}{8\pi I^2}\left[\left(\sum_j K_j(g_j-g_R)\sqrt{(I^2-K^2)}\right)-K\left(\sum_j (g_j-g_R)i_j\right)\right]^2,$$

where

$$K=\sum K_j$$

is the sum of the projections of the individual quasiparticle angular momenta, K_j, on the symmetry axis and i_j is the aligned angular momentum of the jth nucleon of the configuration, having a g factor of g_j. The $B(E2;I\rightarrow I-2)$ values were deduced from the rotational model formula. The intrinsic quadrupole moment has been assumed to be similar to the ground state band ($Q_0=3.8$ e b) [19]. The g factors have been taken from Ward *et al.* [10] and the g_R value has been set to $g_R=Z/A$. In earlier studies [10,11,20,21] in this mass region, the dipole bands have been suggested to be built on four-quasiparticle configurations, because of their large initial aligned angular momentum (Fig. 4). Additional arguments supporting this picture are given later.

The $B(M1)/B(E2)$ ratios resulting from the semiclassical calculations for the configurations $[\nu(h_{11/2}\otimes g_{7/2})]\otimes[\pi(h_{11/2}\otimes d_{5/2}/g_{7/2})]$ (prolate positive parity configuration) and $(\nu h_{11/2}^2)\otimes[\pi(h_{11/2}\otimes d_{5/2}/g_{7/2})]$ (oblate negative parity configuration) are compared to the experimental data in Fig. 6. For the considered deformation, from the Nilsson diagram [22], protons in the $\pi h_{11/2}$ orbital occupy the low $\Omega=1/2$ Nilsson state for a prolate shape and high $\Omega=11/2$ Nilsson state for an oblate shape. The particles in the $\pi d_{5/2}$ orbital occupy the Nilsson states with $\Omega=3/2$ and $\Omega=5/2$ for prolate and oblate shapes, respectively. Similarly the $h_{11/2}$ neutrons occupy the high $\Omega=7/2$ Nilsson state and low $\Omega=3/2$ Nilsson state for prolate and oblate shapes, respectively. Therefore, the prolate configuration is assumed to be built on a $K=7$ configuration and a K value of 8–9 has been assumed for the oblate configuration. The absence of signature splitting, in addition, supports a high-K nature for this band. It is to be mentioned that the K quantum number is only approximately good for the γ-soft Xe-Ba-Ce nuclei.

Before the backbend at spins $(22)\hbar$, the experimental ratios start from a high value of $23.3\pm3.3(\mu_N^2/e^2\mathrm{b}^2)$ and decrease with increasing spin. For the positive parity configuration, the calculation gives a reasonable description of the

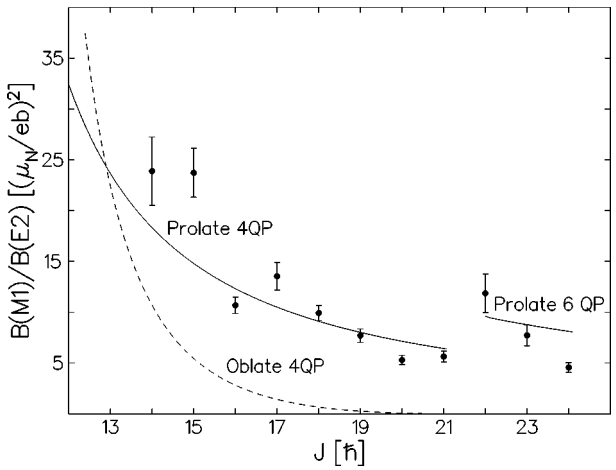

FIG. 6. The experimental $B(M1;I\rightarrow I-1)/B(E2;I\rightarrow I-2)$ ratios of reduced transition probabilities for the dipole band (band 2). Geometric model predictions for the prolate configuration are depicted by the thick, line and the dotted line corresponds to the oblate configuration. The prolate and oblate configurations are described in the text. The input values to the Dönau-Frauendorf formula are $g_R=0.43$, $g^{\pi}_{h_{11/2}}=1.17$, $g^{\pi}_{d_{5/2}}=1.38$, $g^{\nu}_{h_{11/2}}=-0.21$, and $g^{\nu}_{g_{7/2}}=0.21$, $Q_0=3.8$ e b.

experimental data. The high initial data point can be traced to the decrease in the $B(E2)$ value close to the bandhead. This is expected for a high-K band. Additional arguments in support of this configuration are discussed in the following.

(i) The excitation energy of the suggested four-quasiparticle (4qp) band is approximately equal to the sum of the excitation energies of the neutron and proton two-quasiparticle bands (in Fig. 1 bands 1 and 5, respectively). Such 2qp bands are known to occur systematically in the even-even Xe-Ba nuclei [10,21]. The configuration assignment of bands 1 and 5 is suggested to be prolate, $[\nu(h_{11/2}\otimes g_{7/2}]$ and $[\pi(h_{11/2}\otimes d_{5/2}/g_{7/2})]$, respectively. The configuration assignments for these bands are based on the observed signature splittings and on the blocking of the quasiparticle alignments. The proton Fermi surface lies in the beginning of the shell and thus the signature splitting is large for the proton 2qp band. Similarly the neutron Fermi surface is in the middle of the shell; therefore the signature splitting is small for the neutron 2qp band. Band 5 is yrast at high spins and was intensely populated in the present experiment. The detailed discussion of these bands will be reported elsewhere [23].

(ii) The observed alignment in the dipole band close to frequencies 0.5 MeV/$\hbar$ is suggested to be due to the alignment of a second pair of $h_{11/2}$ neutrons. Alignments due to other quasiparticles are predicted to occur at much higher frequencies. This fact is borne out systematically in the neighboring even-even Xe-Ba nuclei [24]. The alignment in band 1 (prolate neutron 2qp) band is observed at a frequency of 0.53 MeV/$\hbar$. This is attributed to $h_{11/2}$ neutrons. Thus the close agreement of the two frequencies suggests a prolate shape for the 4qp dipole band. A comparison of the crossing frequency with the proton 2qp band is not meaningful, as the observed low-frequency alignment is due to the unblocked

first pair of $h_{11/2}$ neutrons. Interestingly, the cranked shell model calculations, with similar deformation parameters, predict this alignment only for a prolate shape. Other quasiparticle alignments are predicted to occur at higher frequencies and are beyond the range of experimental frequencies in the dipole band. The semiclassical estimate for the six quasiparticle prolate configuration is also depicted in Fig. 5 for spins $(22–24)\hbar$. The aligned angular momentum due to the second pair of $h_{11/2}$ neutrons is assumed to be $2\hbar$. The estimates give a reasonable description of the high-spin data, but the limitation of this estimate is the assumption of a fixed K value.

(iii) Using the additivity relations for g factors, the calculated g_k value for this configuration is close to 0.29. If the rotational g factors are assumed to scale as $\sim Z/A$, then $(g_k - g_R)$ will be negative. The rotational model suggests that for the deduced negative mixing ratios δ, the sign of the quadrupole moment would be positive. This further supports the assignment of the prolate configuration.

For the oblate, negative parity configuration $(\nu h_{11/2}^2) \otimes [\pi(h_{11/2} \otimes d_{5/2}/g_{7/2})]$, the semiclassical model fails to describe the angular momentum dependence of the experimental $B(M1;I \rightarrow I-1)/B(E2;I \rightarrow I-2)$ data. An increase or decrease of the quadrupole moment or the K values does not give a better fit to the data. Second, according to the cranked shell model calculations, for the considered oblate configuration the alignment of the second pair of $h_{11/2}$ neutrons is predicted to occur at $\sim 0.30–0.35$ MeV/$\hbar$. However, the observed alignment is at a much higher frequency. In order to construct 4qp oblate bands from analogous 2qp bands, there is no experimental evidence for bands based on oblate two-quasiparticle configurations of the type $[\pi(h_{11/2} \otimes d_{5/2}/g_{7/2})]$ and $[\nu(h_{11/2} \otimes g_{7/2})]$.

V. SUMMARY AND CONCLUSIONS

In summary, the decay out of a high-spin magnetic dipole band has been established for the first time in ^{124}Xe. The $E2/M1$ mixing ratios were determined to ascertain the predominant magnetic character of the dipole gamma transitions. Within the semiclassical model of Dönau and Frauendorf, the experimental branching ratios can be explained assuming a prolate shape based on four different quasiparticles. This was deduced on the basis of ''additivity'' of the corresponding prolate neutron and proton two-quasiparticle bands. The $E2/M1$ mixing ratios and the observed $\nu h_{11/2}$ alignment are consistent with this picture. The semiclassical estimates of the branching ratios were performed for two configurations which have been suggested as possible ones in the neighboring nuclei [10,20,21]. From the present analysis, the prolate configuration gives a good agreement with the experimental data. However, we do not exclude other possibilities. It is to be mentioned here that a thorough analysis is possible only if the parity and the $B(E2)$ and $B(M1)$ transition rates are established. Thus a lifetime experiment is very desirable.

The dipole bands in ^{128}Ba [11] and ^{124}Xe have now been established with good quality data sets from large gamma detector arrays. The deduced small $E2/M1$ mixing ratio for the dipole gamma transitions ascertains the almost pure magnetic character [25]. In both nuclei the dipole bands could be explained as high-K prolate bands rather than as oblate shears bands [21]. Shears bands are a class of high-K bands, *with small deformation*. This enables us to generate states which are obtained by a continuous alignment of the particle-hole spin vectors along the total angular momentum axis by the Coriolis force. It is possible that in the deformed $A \sim 130$ region the shearing mechanism is not the optimal way to generate yrast states. In order to distinguish between the high-K and shears mechanism it is very important to continue the search for such dipole bands with large gamma detector arrays. The present studies highlight the need for complete data sets with an extended band structure to really distinguish between high-K and shears bands. It would be of interest to test the tilted axis cranking (TAC) model for the high-K band suggested in the present analysis. The TAC model is known to be appropriate for high-K bands, as the principle axis cranking does not take into account the effects of rotational perturbation of large spin components onto the symmetry axis. Since the nuclei in this region are known to be axially asymmetric, it would also be interesting to test the inclusion of triaxiality in the TAC calculations.

ACKNOWLEDGMENTS

We thank Dr. Y.R. Shimizu, Dr. A. Gelberg, Dr. R.F. Casten, Dr. J. Gableske, and Dr. J. Eberth for useful discussions. One of us (R.S.C.) is grateful to the Alexander von Humboldt foundation for support. One of us (P.P.) is grateful to BNRF for supporting his research work. The Köln group is grateful to the Tandem accelerator personnel at Risø for smooth operation of the Tandem during the experiment. Many thanks to the Danish Natural Science Research Council for supporting the Tandem-Accelerator-Laboratory in Risø. This work was supported by BMBF under Contract No. O60K 8621 I(O).

[1] R. M. Clark *et al.*, Phys. Lett. B **275**, 247 (1992).
[2] G. Baldsiefen, H. Hübel, W. Korten, D. Metha, N. Nenoff, B. V. Thirumala Rao, P. Willsau, H. Grawe, J. Heese, H. Kluge, K. H. Maier, R. Schubart, S. Frauendorf, and H. J. Maier, Nucl. Phys. **A574**, 521 (1994).
[3] A. Gadea *et al.*, Phys. Rev. C **55**, R1 (1997).
[4] R. S. Chakrawarthy and R. G. Pillay, Phys. Rev. C **55**, 156 (1997).
[5] S. Frauendorf and J. Reif, Nucl. Phys. **A621**, 736 (1997).
[6] S. Frauendorf, Nucl. Phys. **A557**, 259c (1993).
[7] P. M. Walker, G. D. Dracoulis, A. P. Byrne, B. Fabricus, T. Kíbedi, and A. E. Stuchbury, Phys. Rev. Lett. **67**, 433 (1991).

[8] F. Dönau, S. Frauendorf, O. Vogel, A. Gelberg, and P. von Brentano, Nucl. Phys. **A584**, 241 (1995).

[9] R. Wyss, in ''Alignment Processes in ^{122}Ba and Surrounding Nuclei,'' Proceedings of the XXV International Winter Meeting on Nuclear Physics, Bormio, 1987, p. 542.

[10] D. Ward, V. P. Janzen, H. R. Andrews, D. C. Radford, G. C. Ball, D. Horn, J. C. Waddington, K. Johansson, F. Banville, J. Gascon, S. Monaro, N. Nadon, S. Pilotte, D. Prevost, P. Taras, and R. Wyss, Nucl. Phys. **A529**, 315 (1991).

[11] O. Vogel, A. Dewald, P. von Brentano, J. Gableske, R. Krücken, N. Nicolay, A. Gelberg, P. Petkov, A. Gizon, D. Bazzacco, C. Rossi-Alvarez, G. De Angelis, M. De Poli, S. Frauendorf, and F. Dönau, Phys. Rev. C **56**, 1338 (1997).

[12] F. Seiffert, W. Lieberz, A. Dewald, S. Freund, A. Gelberg, A. Granderath, D. Leiberz, R. Wirowski, and P. von Brentano, Nucl. Phys. **A554**, 287 (1993).

[13] L. P. Ekström and A. Nordlund, Nucl. Instrum. Methods Phys. Res. A **313**, 421 (1992).

[14] W. Gast, U. Kaup, H. Hanewinkel, R. Reinhardt, K. Schiffer, K. P. Schmittgen, K. O. Zell, J. Wrzesinski, A. Gelberg, and P. von Brentano, Z. Phys. A **318**, 123 (1984).

[15] I. Wiedenhöver *et al.*, in ''New Spectroscopy and Nuclear Structure 1997,'' Nordic meeting on nuclear physics, Copenhagen, 1997.

[16] G. Lo Bianco, Ch. Protochristov, G. Falconi, N. Blasi, D. Bazzacco, G. de Angelis, D. R. Napoli, M. A. Cardona, A. J. Kreiner, and H. Somacal, Z. Phys. A **359**, 347 (1997).

[17] K. S. Krane and R. M. Steffen, Phys. Rev. C **2**, 724 (1970); **4**, 1419 (1971).

[18] F. Dönau and S. Frauendorf, in *Proceedings of the Conference on High Angular Momentum Properties of Nuclei*, Oak Ridge, 1982, edited by N. R. Johnson (Harwood Academic, New York, 1982), p. 143; F. Dönau, Nucl. Phys. **A471**, 469 (1987).

[19] S. Raman, C. W. Nestor, Jr., S. Kahane, and K. H. Bhatt, At. Data Nucl. Data Tables **42**, 1 (1989); A. Dewald *et al.*, in *Proceedings of the XXV Zakopane School on Physics*, Zakpoane, 1990, edited by J. Styczen and Z. Stachura (World Scientific, Singapore, 1990), Vol. 2, p. 152.

[20] D. B. Fossan, in *Proceedings of the Conference on ''Nuclear Structure in the Nineties*,'' Oak Ridge, Tennessee, 1990, edited by N. R. Johnson (North-Holland, Amsterdam, 1990), Vol. 1, p. 88.

[21] P. Petkov, J. Gableske, O. Vogel, A. Dewald, P. von Brentano, R. Krücken, R. Peusquens, N. Nicolay, A. Gizon, J. Gizon, D. Bazzaco, C. Ross-Alvarez, S. Lunardi, P. Pavan, D. R. Napoli, W. Andrejtscheff, and R. V. Jolos, Nucl. Phys. **A640**, 293 (1998).

[22] P. Petkov, R. Krücken, A. Dewald, P. Sala, G. Böhm, J. Altman, A. Gelberg, P. von Brentano, R. V. Jolos, and W. Andrejtscheff, Nucl. Phys. **A568**, 572 (1994).

[23] I. Schneider *et al.* (unpublished).

[24] R. Wyss, A. Granderath, R. Bengtsson, P. von Brentano, A. Dewald, A. Gelberg, A. Gizon, J. Gizon, S. Harissopoulos, A. Johnson, W. Leiberz, W. Nazarewicz, J. Nyberg, and K. Schiffer, Nucl. Phys. **A505**, 337 (1989).

[25] I. Weidenhöver, O. Vogel, H. Klein, A. Dewald, P. von Brentano, J. Gableske, R. Krücken, N. Nicolay, A. Gelberg, P. Petkov, A. Gizon, J. Gizon, D. Bazzaco, C. Rossi-Alvarez, G. de Angelis, S. Lunardi, P. Pavan, D. R. Napoli, S. Frauendorf, F. Dönau, R. V. F. Janssens, and M. P. Carpenter, Phys. Rev. C **58**, 721 (1998).